PCCP

Accepted Manuscript

ROYAL SOCIETY OF CHEMISTRY

www.rsc.org/pccp

Journal Name

RSCPublishing

COMMUNICATION

Cite this: DOI: 10.1039/xoxxoooooox
Received ooth January 2012,
Accepted ooth January 2012
DOI: 10.1039/xoxxoooooox
www.rsc.org/

Dynamic interface charge governing the current-voltage hysteresis in perovskite solar cells†

Huimin Zhang,[a] Chunjun Liang,*[a] Yong Zhao,[a] Mengjie Sun,[a] Hong Liu,[a] Jingjing Liang,[a] Dan Li,[a] Fujun Zhang[a] and Zhiqun He*[a]

The accumulation of mobile ions causes space charge at interfaces in perovskite solar cells. There is a slow dynamic process of ion redistribution when the bias is changed. The interface charge affects the band bending and thus the photocurrent of the solar cells. Consequently the dynamic process of the interface charge governs the current-voltage hysteresis. Very low interface charge density leads to hysteresis-free devices.

Despite the rapid progress of perovskite solar cells (PSCs) based on the organic–inorganic halide perovskites[1-10], the fundamental problem, i.e. the origin of current-voltage hysteresis, is still a challenge in the field. The current–voltage (J–V) hysteresis refers to the phenomenon that the shape of the J–V curve varies depending on the scan direction, range, and rate of the scan voltage during measurements as well as the condition before the measurements. Hysteresis in PSCs has been speculated to originate from trapping/de-trapping of charge carriers [11, 12], changes in absorber or contact conductivity[13], ferroelectricity[11, 14-16]and ion migration[11, 16-20]. It was observed that hysteresis-free J–V curves can be obtained at both extremely fast and slow voltage scan rates, suggesting that quasi-steady states exist and a slow transient process gives rise to the hysteresis[21]. Recent works[22, 23] indicated that large amount of mobile ions exist in the perovskite layer. The accumulation of the mobile ions at the interfaces between the perovskite and the other layers results in large quantity of interface charge, which significantly changes the band bending of the semiconductor near the interface[23].

In this work, we investigated the correlation between the dynamic change of the interface charge and the photocurrent in PSCs. The results indicate that the existence of the interface charge significantly affects the carrier collection efficiency of PSCs. Consequently under fast changing bias the dynamics of the interface charge governs the current-voltage hysteresis. Finally we show that the degree of the hysteresis is closely related to the magnitude of the interface charge. Very low interface charge density leads to hysteresis-free devices.

PbI_2 (99.999%, Sigma-Aldrich) and $PbCl_2$ (99.999%, Sigma-Aldrich) with 1:1 mole ratio were dissolved in DMF (1mol/ml) and CH_3NH_3I (MAI) (>99.9%, HeptaChroma) was dissolved in 2-propanol. To ensure MAI, $PbCl_2$ and PbI_2 were fully dissolved, both solutions were heated at 70 ℃ for 30 min before use. The device architecture is ITO/PEDOT:PSS/ $MAPbI_xCl_{3-x}$ /$PC_{61}BM$/Al, and the active area is 0.038 cm^2. PEDOT:PSS (Baytron-P4083) was spin-cast onto the clean surface of the ITO substrates at 3000 rpm for 40 s and then thermally annealed on a hot plate at 120 ℃ for 30 min in air. In a nitrogen-filled glove box, the solution of PbI_2 and $PbCl_2$ was spin-coated onto the PEDOT:PSS layer at 4000 rpm for 15 s and then annealed at 70 ℃ for 15 min. After drying, the MAI solution in 2-propanol (40 mg/ml) was spin-coated onto the PbICl layer at 3000 rpm for 5 s and then annealed at 70 ℃ for 30 min to form the perovskite $MAPbI_3Cl_{3-x}$. $PC_{61}BM$ (in chlorobenzene) was then spin-coated onto the perovskite layer at 3000 rpm for 40 s. The $PC_{61}BM$ concentration of 20 mg/ml lead to the $PC_{61}BM$ thickness of 40 nm. Finally, the samples were moved into a vacuum chamber for aluminium deposition. The thickness of the perovskite is ~370 nm, as measured with an Ambios XP-2 profilometer. The J–V characteristics were recorded by a Keithley (and Agilent) source meter under an illumination of AM 1.5G 100 mW/cm^2 from an Abet 2000 solar simulator.

The interface charge is the accumulated mobile ions at the interface under electric field. The interface charge is always accompanied by screen charge on the electrode. After applying a constant bias on the device for a long period of time, the density of the interface charge is fixed, and we define this condition as quasi-steady state in the following discussion. Stronger field leads to higher density of interface charge. When the applied bias is changed, for example, from V_a to V_b, the quasi-steady-state density of the interface charge will change accordingly. However, because of the slow redistribution process of the mobile ions, it takes some time to reach the final quasi-steady state at V_b. Therefore there is a slow dynamic process of ions redistribution if the applied voltage is changed from one value to another. The dynamics of the ions-related interface charge can be observed at dark and short-circuit condition because electron and hole current are zero in this condition.

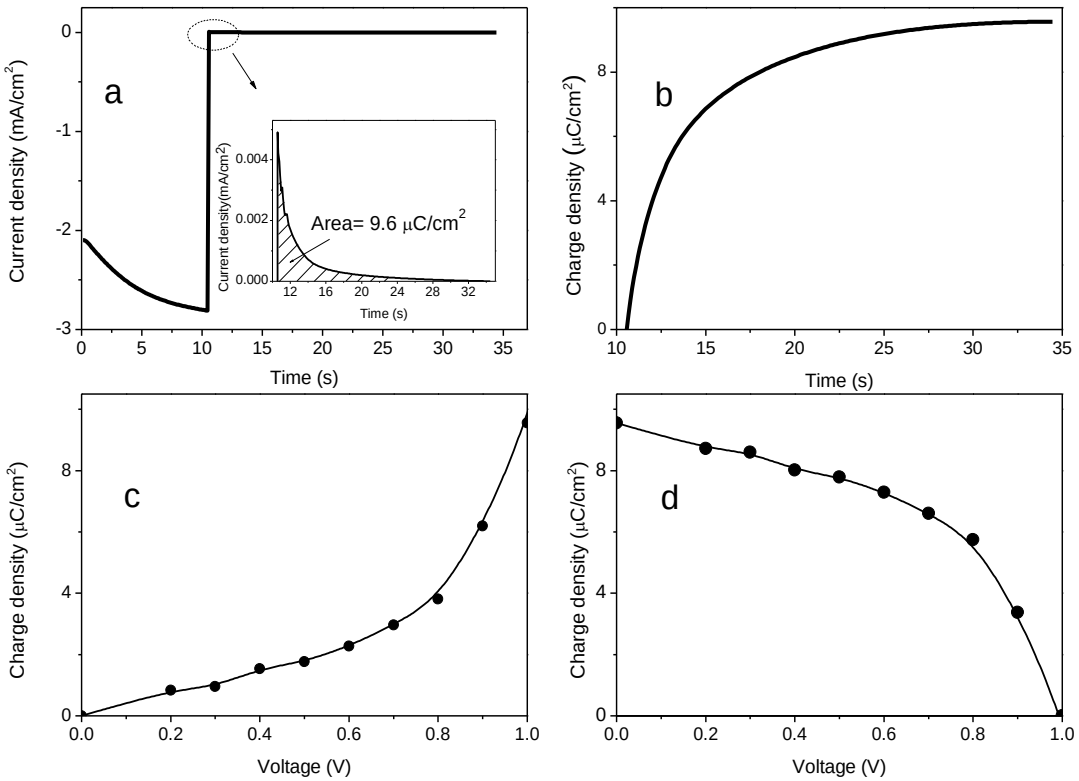

Figure 1. Dynamics of the interface charge. a, Under dark condition a bias of 1.0 V was applied on the device for 10 s. The device was then kept at a short circuit condition to observe the non-zero current. The inset shows the current. **b,** The time integral of the current density shows the dynamic change of the interface charge after the applied voltage is changed from 1.0 V to zero. **c,** The difference of quasi-steady-state charge density between different bias and the zero bias. **d,** The quasi-steady-state density of interface charge at various bias.

The dynamic change of the interface charge from 1.0 V to 0 V in the PSCs with a 40-nm $PC_{61}BM$ is illustrated in Figure 1. A bias of 1.0 V was applied on the device for 10 s to reach the quasi-steady state at 1.0 V. After removal of the 1.0 V bias (Figure 1a), a small reverse current appears and decays (Figure 1a, inset), indicating that the interface charge is changing. The time integral of the short-circuit current indicates the dynamic change of the interface charge (Figure 1b). The interface charge changes quickly at the beginning, and then gradually stabilizes in a timescale of ~10 s. The finally stabilized value is 9.6 μC/cm^2, which is the difference of the quasi-steady-state interface charge density between 1.0 V and zero bias (short-circuit condition). Similarly, the difference of quasi-steady-state charge density between other bias and the zero bias was measured (Figure 1c). The result indicates that when the bias is changed it will need ~10 s to reach the final quasi-steady state. Therefore in the following discussion, we will apply the constant bias V_a for 10 s on the device if we want to achieve the quasi-steady state at V_a.

Although the difference of the quasi-steady-state charge density between a given bias V_a and the zero bias is obtained (Figure 1c), the actual quasi-steady-state interface charge density at V_a is not known because we still need to figure out the interface charge density at zero bias. A reasonable estimation is that under strong illumination and at the bias of open-circuit voltage (Voc) the electric field in the semiconductor is much lower (even close to zero) than that at short-circuit condition. Therefore as a first approximation we assume that at Voc bias the interface charge density is zero. Thus the density of the quasi-steady-state interface charge at zero bias can be estimated from the difference between the charge density at 0 V and at open-circuit voltage. Our device shows a Voc of ~1.0 V under one Sun illumination. Therefore in the following discussion we assume that at the bias of 1.0 V the interface charge density is zero, and at zero bias the interface charge density is 9.6 μC/cm^2, which is the difference between the charge density at zero bias and at 1.0 V. This assumption and the measured difference of the charge density between V_a and zero bias (Figure 1c) lead to the estimated quasi-steady-state interface charge density at the given bias V_a (Figure 1d). The quasi-steady-state charge density at Voc bias (1.0 V) is zero, and it increase continuously with decreasing voltage.

Under dark condition, the observed non-zero short-circuit current leads to the dynamic change of the interface charge (Figure 2a). Under light illumination we investigated the dynamic change of the photocurrent. Figure 2b shows the dynamic change of the short-circuit current (Isc) under illumination after the device is switched from different initial quasi-steady state to short-circuit state. Taking the initial quasi-steady state of 1.0 V as an example: under one sun illumination, a bias of 1.0 V (Voc) was applied on the device for 10 s to reach the quasi-steady state at 1.0 V; the device was then kept at short-circuit condition to observe the photocurrent (Figure 2b, dark diamond). The photocurrent decrease quickly at the beginning, and then gradually stabilizes in a timescale of ~ 10 s. The dynamic change of the photocurrent is in the same manner and the same time scale as that of the interface charge (Figure 2a). The correlation strongly suggests that the transient process of the interface charge leads to the dynamic change of the photocurrent. It also suggests that higher interface charge density results in lower photocurrent. This

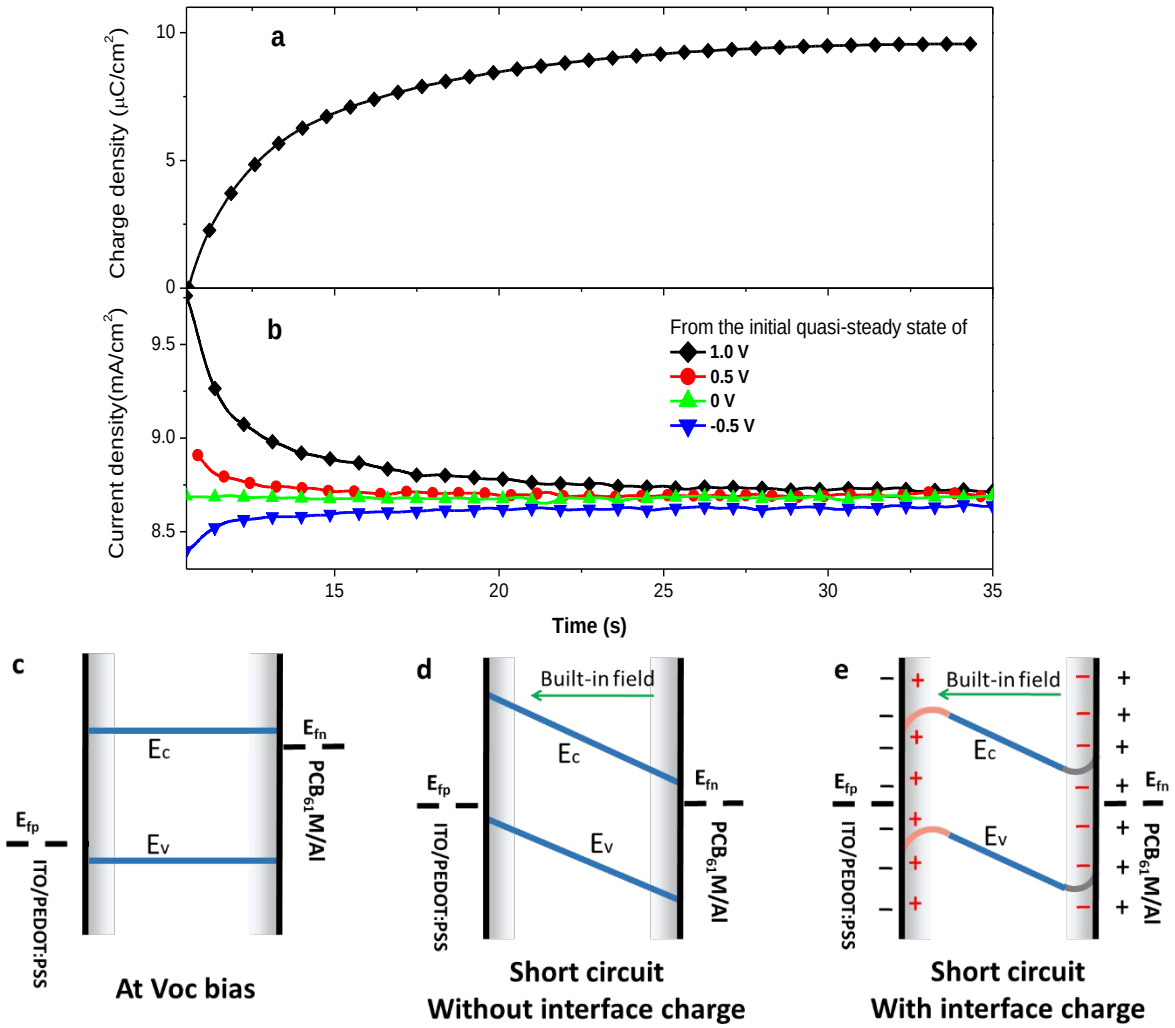

Figure 2. Interface charge changes band bending and thus influences the photocurrent of PSCs. a, Dynamic change of the interface charge after the bias is switched from 1.0 V to zero (Figure 1b is moved here). **b,** Dynamic change of the short-circuit current (Isc) under illumination after the device is switched from different initial quasi-steady state to short-circuit state. **c-e,** Schematic energy band diagrams at different condition. **c,** at the quasi-steady state of Voc voltage (1.0 V). **d,** at the beginning moment after the device bias is switched from 1.0 V to zero. **e,** at quasi-steady state of zero bias. Interface charge and screen charge are represented in red and black,

conclusion is further confirmed in the results of different initial state, which indicate that the initial quasi-steady state has significant influence on the transient of the photocurrent. It clearly shows that the initial state with higher positive voltage, for example 1.0 V, leads to higher beginning Isc than the stabilized Isc, and the initial state with lower voltage, for example -0.5 V, leads to lower beginning Isc (Figure 2b, blue downward triangle). We note that the quasi-steady state with high voltage have low density of interface charge (Figure 1d). Thus these results consistently indicate that the density of the interface charge significantly affects the photocurrent. The lower the interface charge density the higher the photocurrent, and vice versa.

The above observations are consistent with the recently revealed mechanism that the existence of the interface charge changes the band bending near the interfaces[23] and thus affects the carrier collection efficiency of the device. Taking the initial quasi-steady state of Voc bias (1.0 V) as an example: there is no interface charge because the intensity of the electric field is close to zero in the perovskite layer at this condition (Figure 2c). When the device is quickly changed to short-circuit state, the bands of the semiconductor become tilted because of the built-in field in the device. At the very beginning moment after the switch, there is no interface charge in the device (Figure 2d). However the built-in field drifts the mobile ions towards the interface. The direction of the built-in field is from $PC_{61}BM$ to PEDOT:PSS. Thus positive interface charge gradually accumulates at the PEDOT:PSS interface and negative charge accumulates at $PC_{61}BM$ interface (Figure 2e). Our previous work shows[23] that positive interface charge leads to downward band bending near the interface and negative interface charge leads to upward band bending (Figure 2e). The downward band bending hinders hole collection at PEDOT:PSS interface, and the upward band bending hinders electron collection at $PC_{61}BM$ interface. Therefore at the voltage below Voc, the resulting interface charge, positive at the PEDOT:PSS interface and negative at the $PC_{61}BM$ interface, is detrimental for carrier collection. Thus lower density of interface charge leads to higher photocurrent and vice versa. This mechanism consistently explains the dynamic change of photocurrent when the device is switched from different initial quasi-steady states to short-circuit condition (Figure 2b).

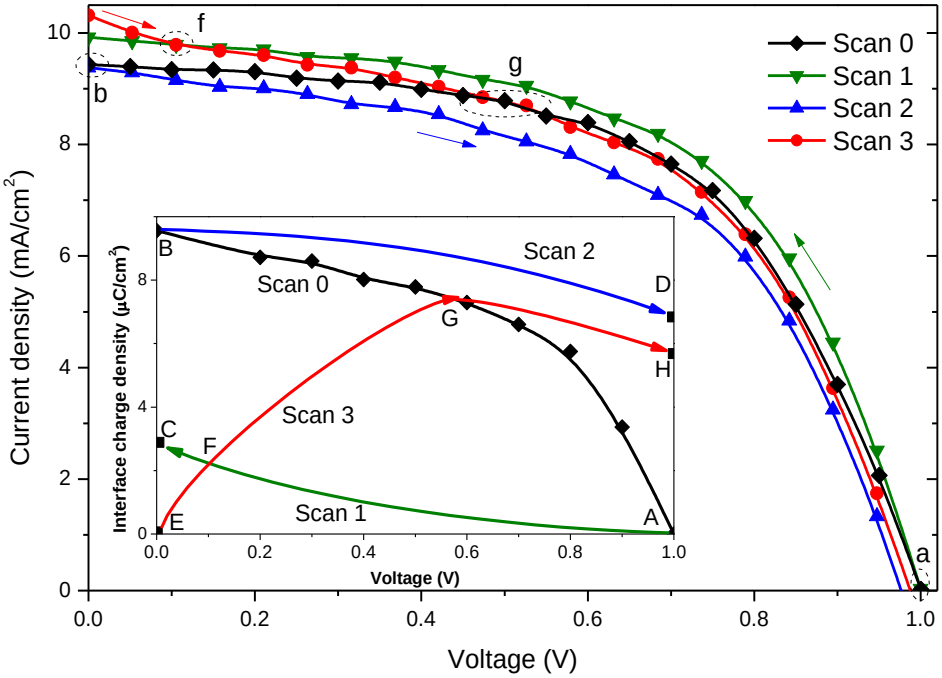

Figure 3. The correlation between the J–V hysteresis and the dynamic change of the interface charge shows that the dynamic process of the interface charge governs the J–V hysteresis. Scan 0 is a slow scan with the delay time of 10 s. **Scan 1, 2 and 3** are fast scans with a scan rate of 0.5 V/s. **Scan 1** is from 1.0 V to 0 V, and the initial state is the quasi-steady state of 1.0 V. **Scan 2** is from 0 V to 1.0 V, and the initial state is the quasi-steady state of 0 V. **Scan 3** is from 0 V to 1.0 V, and the initial state is the quasi-steady state of 1.0 V. The inset shows the dynamic process of the interface charge during the scans. In the inset the scatters are measured and the arrow lines are sketched.

With several specially designed scan routes, we show that the J–V hysteresis (Figure 3) is governed by the dynamics of the interface charge under changing bias (Figure 3 inset). Scan 0 is a very slow scan, in which the delay time for every measuring point is 10 s. As expected, the J–V curve is hysteresis-free (Figure 3, black diamond) because the interface charge can reach quasi-steady state at each measuring point regardless of the scan direction. Scan 1, 2 and 3 are fast scans with a scan rate of 0.5 V/s. In fast scan because the interface charge cannot reach the quasi-steady state in the short period of time, there is a dynamic process of the interface charge, which is determined by the initial state right before the scan and the scan direction and rate during the scan. Scan 1 represents the scan from 1.0 V to 0 V, and the initial state is the quasi-steady state of 1.0 V (we applied the bias of 1.0 V on the device for 10 s right before the scan). Because of the fast scan, the density of the interface charge changes very little and keeps significantly lower than the quasi-steady-state value in the whole scanning process. Consequently, the photocurrent of Scan 1 is significantly higher than that of Scan 0. Scan 2 represents the scan from 0 V to 1.0 V, and the initial state is the quasi-steady state of 0 V (a bias of 0 V was applied on the device for 10 s before the scan). This scan begins with a high density of interface charge. And because of the fast scan, the interface charge density keeps higher than the quasi-steady-state value (Scan 0), leading to the apparently lower photocurrent than the quasi-steady-state photocurrent. Scan 3 is an interesting scan rout, which is also from 0 V to 1.0 V (the same as Scan 2), but the initial state is the quasi-steady state of 1.0 V (a bias of 1.0 V was applied on the device for 10 s before the scan). At the beginning of this scan, the density of interface charge is zero, and it increases continuously to pass through Scan 1 and Scan 0, and then decrease, because the density of interface charge always tends to reach the quasi-steady-state value. It has two intersections with the other scan curves at point F and G (Figure 3 inset). Interestingly and importantly, the J–V curve begins with the highest photocurrent at 0 V, and it passes through Scan 1 and Scan 0 as expected. There are four intersections, A, B, F and G, in the density-voltage curves (Figure 3 inset). These intersections lead to the corresponding intersection points, a, b, f and g, in the J–V curves, respectively, because at the same bias and the same density of interface charge the photocurrent should be the same. We note that all of the J–V curves in Figure 3 were measured in the same device, and the results are repeatable. These results clearly indicate that the dynamics of interface charge governs the J–V hysteresis of the PSCs.

The thickness of the $PC_{61}BM$ layer significantly affects the interface charge density and thus the degree of the J–V hysteresis (Figure 4). The interface charge density at short-circuit condition reaches 131.4 μC/cm^2 at the $PC_{61}BM$ thickness of 10 nm (Figure 4a), and it significantly decreases to 0.3 μC/cm^2 at the $PC_{61}BM$ thickness of 90 nm (Figure 4c). As expected, the J–V hysteresis is very severe in the former device, while the J–V curve is hysteresis-free in the latter device. This result further confirms that the dynamic change of the interface charge is the origin of the J–V hysteresis. We note that the hysteresis-free J–V curves were previously reported in the PSCs with a very similar device configuration[24]. The detailed mechanism determining the density of the interface charge needs further investigation. It is likely that at short-circuit condition the density of the interface charge is determined by the electrostatic effect of the mobile ions in the perovskite and the screening charge on the electrode. If it can be assumed that the positive screening charge is not in close proximity to the negative interface charge (Figure 2e), and the carrier selective $PC_{61}BM$ layer somehow acts as dielectrics between them, it is understandable that a thick 'dielectric'

layer would lead to a low surface charge density (like a plate capacitor).

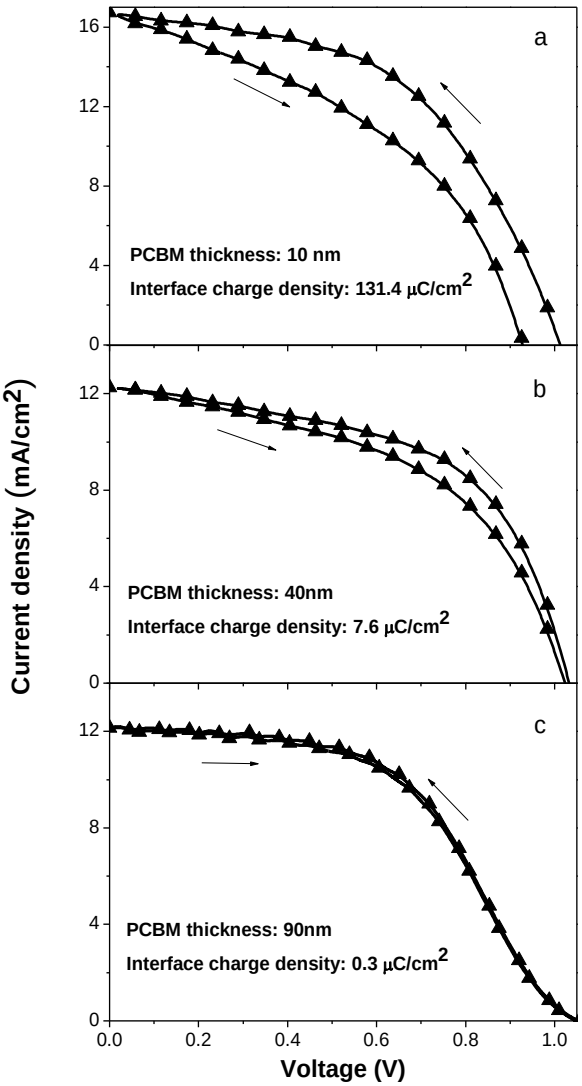

Figure 4. The influence of $PC_{61}BM$ thickness on the interface charge and the J–V hysteresis. Very low interface charge density leads to hysteresis-free J–V characteristics (panel c). The scan rate is 0.5 V/s.

Conclusions

In conclusion, the accumulation of mobile ions in the hybrid perovskites causes space charge at interfaces. Under quasi-steady state (under a constant bias for a long period of time) the density of the interface charge is fixed and is determined by the intensity of the electric field. When the applied bias is changed, the quasi-steady-state density of the interface charge will change accordingly. However, due to the slow redistribution process of the mobile ions, it takes some time (~10 s) to reach the final quasi-steady state. When the voltage scan rate is slow (delay time ≥ 10 s), the device can reach the quasi-steady state at every measuring point. However, when the scanning voltage changes rapidly, the device cannot reach the quasi-steady state in the measuring process. The dynamics of the interface charge under fast scan rate depends on the initial charge density before the scan and the conditions (scan direction and scan rate) during the scan.

The results show that the existence of the interface charge significantly affects the photocurrent. The lower the interface charge density the higher the photocurrent. The results is consistent with the mechanism that the existence of the interface charge changes the band bending near the interface and thus significantly affects the carrier collection efficiency. At the voltage below Voc, the resulting interface charge, positive at the PEDOT:PSS interface and negative at the $PC_{61}BM$ interface, is detrimental for carrier collection. Therefore lower interface charge density leads to higher photocurrent and vice versa.

The aforementioned mechanism suggests that the dynamic change of the interface charge leads to J–V hysteresis. Indeed, with several specially designed scan routes, we show that the J–V hysteresis of the device is governed by the dynamics of the interface charge under changing bias. Finally we show that the thickness of the carrier-selective layer ($PC_{61}BM$) significantly affects the interface charge density and thus the J–V hysteresis in PSCs. In the device with a thick $PC_{61}BM$ layer (90 nm) very low interface charge density ($0.3\mu C/cm^2$) leads to hysteresis-free J–V characteristics.

Acknowledgments

The authors acknowledge the financial support from the National Natural Science Foundation of China (No. 11474017, 21174016 and 60776039), the Research Fund for the Doctoral Program of Higher Education of China (No. 20120009110031), and the Fundamental Research Funds for the Central Universities (No. 2013JBZ004, 2013JBM102).

Notes and references

[a] Key Laboratory of Luminescence and Optical Information, Ministry of Education, School of Science, Beijing Jiaotong University, Beijing 100044, China. E-mail: chjliang@bjtu.edu.cn and zhqhe@bjtu.edu.cn

† Electronic Supplementary Information (ESI) available. See DOI: 10.1039/c000000x/

1. A. Kojima, K. Teshima, Y. Shirai and T. Miyasaka, *J Am Chem Soc*, 2009, **131**, 6050-6051.
2. J. Burschka, N. Pellet, S.-J. Moon, R. Humphry-Baker, P. Gao, M. K. Nazeeruddin and M. Gratzel, *Nature*, 2013, **499**, 316-319.
3. D. Liu and T. L. Kelly, *Nat Photon*, 2014, **8**, 133-138.
4. H. Zhou, Q. Chen, G. Li, S. Luo, T. B. Song, H. S. Duan, Z. Hong, J. You, Y. Liu and Y. Yang, *Science*, 2014, **345**, 542-546.
5. P. Docampo, F. C. Hanusch, S. D. Stranks, M. Döblinger, J. M. Feckl, M. Ehrensperger, N. K. Minar, M. B. Johnston, H. J. Snaith and T. Bein, *Advanced Energy Materials*, 2014, **4**, n/a-n/a.

6. J. M. Ball, M. M. Lee, A. Hey and H. J. Snaith, *Energy & Environmental Science*, 2013, **6**, 1739-1743.
7. S. Sun, T. Salim, N. Mathews, M. Duchamp, C. Boothroyd, G. Xing, T. C. Sum and Y. M. Lam, *Energy & Environmental Science*, 2014, **7**, 399.
8. Z. Xiao, C. Bi, Y. Shao, Q. Dong, Q. Wang, Y. Yuan, C. Wang, Y. Gao and J. Huang, *Energy & Environmental Science*, 2014, **7**, 2619-2623.
9. S. Ryu, J. H. Noh, N. J. Jeon, Y. C. Kim, S. Yang, J. W. Seo and S. I. Seok, *Energy & Environmental Science*, 2014, **7**, 2614-2618.
10. M. M. Lee, J. Teuscher, T. Miyasaka, T. N. Murakami and H. J. Snaith, *Science*, 2012, **338**, 643-647.
11. H. J. Snaith, A. Abate, J. M. Ball, G. E. Eperon, T. Leijtens, N. K. Noel, S. D. Stranks, J. T.-W. Wang, K. Wojciechowski and W. Zhang, *The Journal of Physical Chemistry Letters*, 2014, **5**, 1511-1515.
12. T. a. W. Heiser, E. R., *Phys. Rev. B*, 1998, **58**, 3893.
13. D. L. Staebler and C. R. Wronski, *Journal of Applied Physics*, 1980, **51**, 3262.
14. J. M. Frost, K. T. Butler, F. Brivio, C. H. Hendon, M. van Schilfgaarde and A. Walsh, *Nano Lett*, 2014, **14**, 2584-2590.
15. F. Brivio, A. B. Walker and A. Walsh, *APL Materials*, 2013, **1**, 042111.
16. A. Dualeh, T. Moehl, N. Tétreault, J. Teuscher, P. Gao, M. K. Nazeeruddin and M. Grätzel, *Acs Nano*, 2013, **8**, 362-373.
17. K. Yamada, K. Isobe, E. Tsuyama, T. Okuda and Y. Furukawa, *Solid State Ionics*, 1995, **79**, 152-157.
18. R. G. D. D. S. Albin, S. C. Glynn, J. A. del Cueto and W. K. Metzger, ed. J. H. W. a. D. T. T. N. G. Dhere, 2009, p. 74120I.
19. J. Mizusaki, K. Arai and K. Fueki, *Solid State Ionics*, 1983, **11**, 203-211.
20. I. Lyubomirsky, M. K. Rabinal and D. Cahen, *Journal of Applied Physics*, 1997, **81**, 6684.
21. E. L. Unger, E. T. Hoke, C. D. Bailie, W. H. Nguyen, A. R. Bowring, T. Heumüller, M. G. Christoforo and M. D. McGehee, *Energy Environ. Sci.*, 2014, **7**, 3690-3698.
22. Z. Xiao, Y. Yuan, Y. Shao, Q. Wang, Q. Dong, C. Bi, P. Sharma, A. Gruverman and J. Huang, *Nature materials*, 2014.
23. Y. Zhao, C. Liang, H. M. Zhang, D. Li, D. Tian, G. Li, X. Jing, W. Zhang, W. Xiao, Q. Liu, F. Zhang and Z. He, *Energy & Environmental Science*, 2015.
24. O. Malinkiewicz, C. Roldán-Carmona, A. Soriano, E. Bandiello, L. Camacho, M. K. Nazeeruddin and H. J. Bolink, *Advanced Energy Materials*, 2014, **4**, 1400345.

